

# MIMO Free Space Optical Communications in Turbid and Turbulent Atmosphere (Invited Paper)

Zeinab Hajjarian and Jarir Fadlullah

The Pennsylvania State University Department of Electrical Engineering, University Park, PA. 16802, USA  
Email: {zvh116, jmf114} @psu.edu

Mohsen Kavehrad (FIEEE)

The Pennsylvania State University, Department of Electrical Engineering, University Park, PA. 16802, USA  
e-mail [mkavehrad@psu.edu](mailto:mkavehrad@psu.edu)

**Abstract**— Free Space Optical (FSO) communications is the only viable solution for creating a three-dimensional global communications grid of inter-connected ground and airborne nodes. The huge amount of data exchange between satellites and ground stations demands enormous capacity that cannot be provided by strictly regulated, scarce resources of the Radio Frequency (RF) spectrum. Free Space Optical (FSO) communications, on the other hand, has the potential of providing virtually unlimited bandwidth. Furthermore, due to the spatial confinement of laser beams, such links are very secure. In other words, security is guaranteed at the physical layer. However, the promised enormous data rates are only available under clear weather conditions, and atmospheric phenomena such as clouds, fog, and even turbulence can degrade the performance, dramatically. While turbid media such as clouds and aerosols cause pulse broadening in space and time, turbulence presents itself as scintillation and fading. Hence, to exploit the great potentials of FSO at its best under all weather conditions, prudent measures must be taken in the design of transmitter and receiver. More specifically, multiple transmitters and receivers can be used to combat the turbulence-induced fading and to compensate for pulse attenuation and broadening caused by scattering. In this paper, Multiple-Input Multiple-Output (MIMO) transmitter and receiver designs for FSO communications are investigated and the achievable performance improvements are discussed.

**Index Terms**— Free Space Optical (FSO), Multi-Input Multi-Output (MIMO), Point Spread Function (PSF), Scattering, Scintillation.

## I. INTRODUCTION

Free Space Optical (FSO) communication offers a great potential for creating a three-dimensional global communications grid. This is basically due to the ease of deployment of FSO links, unregulated frequency band, and the enormous available bandwidth. Moreover, spatial confinement of laser beams significantly reduces the power loss, and the possibility of interference or interception. All these benefits are viable only under ideal

channel conditions, and atmospheric phenomena such as clouds, fog, aerosols, and even turbulence can severely degrade the performance. While clouds and aerosols scatter the laser beam and give rise to optical pulse attenuation and broadening in space and time, turbulence manifests itself as perturbations in the amplitude and phase of received signal.

To mitigate the deleterious effects of scattering and turbulence, multiple transmitters and receivers can be used. Hence, it would be possible to benefit from spatial diversity and receive multiple independent copies of the same signal. The effectiveness of Multiple-Input Multiple-Output (MIMO) systems in combating the log-normal amplitude fading has been demonstrated in the published literature [1-3]. However, little effort has been made to analyze the possible excess gain obtained using a MIMO system to ameliorate the impact of phase-front distortion [4]. In this paper, we consider both amplitude and phase distortions and show how performance is degraded compared to an Additive White Gaussian Noise (AWGN) channel. Then, using average Bit Error Rate (BER) as a performance metric, possible improvements achieved using a MIMO communications scheme is investigated. The remainder of this paper is organized as follows. In section 2, a channel model is presented. Section 3 demonstrates the system design. In section 4 simulations results are presented and compared under different channel conditions. Finally, section 5 concludes the paper.

## II. CHANNEL MODEL

The first step in designing a communications system in any medium is to know what happens to a wave or a signal as it travels through that medium. This task is usually accomplished by measuring or simulating the channel impulse response. In an atmospheric channel, we have two principal phenomena: scattering and turbulence-induced scintillation. Assuming that these two phenomena are independent, it would be possible to investigate the attributes of each in the total system impulse response. Note that, this is a simplifying assumption, which may not be accurate. However, this is the only way that makes this analysis mathematically tractable. Later in this paper, we will see that such an

assumption is valid for a communications scenario, since due to small Field-Of-View (FOV) of the receiver, multiple scatterings give rise to a sole attenuation factor in the system impulse response. The next two subsections elaborate more on scattering and turbulence.

*A. Mie theory and the scattering impulse response*

Laser beam propagation through clouds, fog, and aerosols is basically a multiple scattering problem. Clouds are made of water droplets with sizes comparable to the optical wavelengths. Hence, Mie theory of scattering governs laser beam interaction with cloud particles. This theory is “an application of Maxwell’s equations to the problem of a homogeneous sphere radiated by a plane wave from a single direction” [5].

In airborne laser communications, transmitter launches a laser pulse, which can be modeled as a large body of photons. Each of these photons proceeds into the medium until it interacts with a particle. At this point, the photon is deflected and its direction of propagation changes. The photon continues in this new direction until it collides with the next particle. According to Mie theory, scattering direction in three-dimensional space is given by a probability distribution function (PDF) known as the Volume Scattering (or Phase) Function. In other words, phase function is the PDF of solid angle  $\psi = (\theta, \varphi)$  and is normalized so that its integral over the entire solid angle is unity [6, 7], i.e.:

$$\int_{4\pi} P(\theta)d\psi = \int_0^{2\pi} \int_0^{\pi} P(\theta) \sin(\theta)d\theta d\varphi = 1 \quad (1)$$

Since the azimuth scattering angle is uniformly distributed in  $[0, 2\pi]$ , phase function can be plotted only with respect to  $\theta$ . Fig. 1 shows the scattering phase function for different types of clouds. These phase functions are obtained by substituting the modified gamma distribution for radius density of cloud particles in equations extracted from Mie theory for poly-dispersed phase function [6, 8].

Assuming a homogeneous scattering medium, the scattering distance, i.e. the distance between two successive scattering events is an exponential random variable distributed as:

$$P(d) = \frac{1}{D_{scat}} e^{(-d/D_{scat})}, \quad (2)$$

where  $D_{scat} = 1/\beta_{scat}$ , and  $\beta_{scat}$  is the scattering coefficient. In photon-particle interactions, there is always a possibility that the photon is absorbed by a particle. This probability is given by the ratio of absorption and extinction coefficients, i.e.,  $P_{abs} = \beta_{abs} / \beta_{ext}$ , however, this probability is very low for clouds since the absorption coefficient is very small compared to the extinction coefficient.

Currently, most FSO communications systems use Intensity Modulation with Direct Detection (IM/DD) due to the complications associated with phase and frequency modulation [2]. In this paper, we use On-Off Keying

(OOK) modulation because of its simplicity. Hence, the channel impulse response is the received intensity, when an impulse is launched from the transmitter. To measure the channel impulse response, we use the Monte-Carlo Ray Tracing (MCRT) algorithm. This algorithm basically tracks the paths of a large number of photons (chosen as 1 million in our simulations) through the scattering medium, and finds the spatial and temporal distribution of photons at the receiver side. Then, considering the receiver aperture area and Field-Of-View (FOV), the system impulse response can be computed.

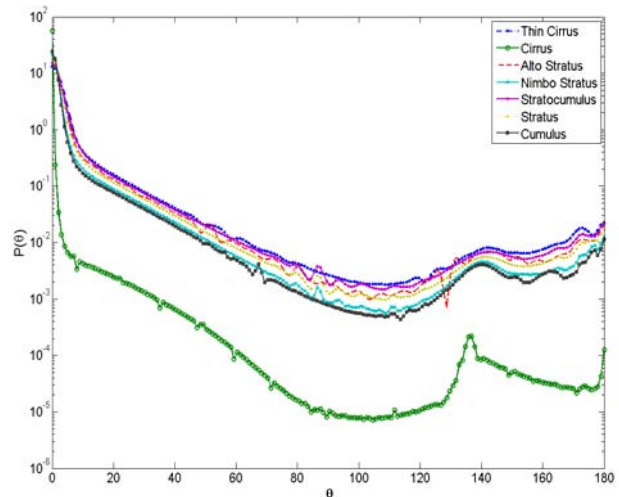


Figure 1. Phase function of different types of clouds.

Multiple scatterings will broaden the collimated beam and attenuate the signal. Furthermore, the collimated beam will break up and arrive at the receiver from many different angles or spatial modes. This phenomenon is usually called the “shower glass” effect [9]. Depending on the FOV, receiver may or may not collect the scattered light rays.

The spatial and temporal system impulse responses are composed of two components: coherent and diffuse [10, 11]. The coherent component of impulse response is the Line-Of-Sight (LOS) portion of transmitted intensity which is attenuated according to the Beer-Lambert law as [6]:

$$I_{coh} = I_0 e^{-\tau} = I_0 e^{-\beta_{sca} L}, \quad (3)$$

where  $\tau$  is the average number of scattering events over a length  $L$  of the cloud, and is defined by multiplying the cloud scattering coefficient  $\beta_{sca}$  ( $km^{-1}$ ) by its physical length,  $L$ , in km and hence has no units. Since this portion of the impulse response is an attenuated version of the original impulse, it is not broadened in time or space. The diffuse component, on the other hand, is composed of the multiple-scattered photons which are dispersed angularly, spatially, and temporally. This component gives rise to pulse broadening in space and time.

The actual shape and width of system impulse response depends on physical aperture size and FOV of

the receiver. In Fig. 2, impulse responses of systems operating in cumulus clouds of various optical thickness values are shown, where a hypothetical aperture of infinite extent is used to collect the transmitted light. To ease the comparison of impulse responses, y-axis is in log-scale. One can see that the impulse response broadens with optical thickness. Fig. 3 shows impulse responses for the same optical thickness values for a receive aperture size of 20 cm diameter. It is apparent that pulse broadening is much less in this case due to the fact that most received power is composed of either “ballistic” (LOS) or “snake” (highly forward-scattered) photons. While percentage of snake photons (compared to the total number of received photon) increases with optical thickness, peak value of impulse response reduces exponentially. The curves in Figs. 2 and 3 are obtained using MCRT [8].

To increase the amount of received power, one can increase the receiving aperture size and FOV and collect some of the diffuse power as well. This excess power, however, manifests itself as a long tail in the impulse response, and hence gives rise to intersymbol interference (ISI), which in turn reduces the achievable bit rate.

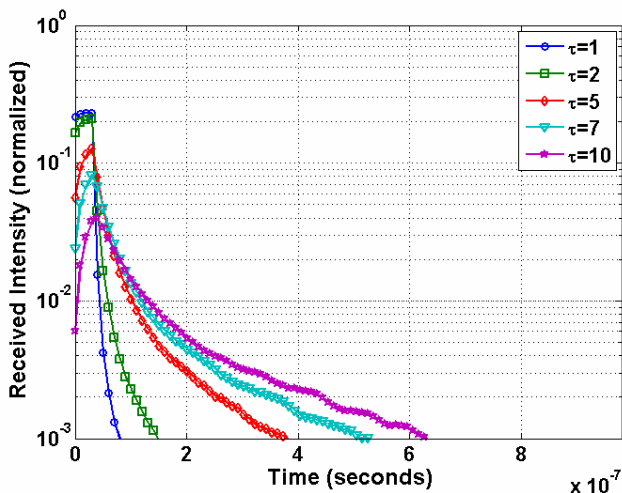


Figure 2. Impulse response of a system with an infinite aperture for different optical thickness values.

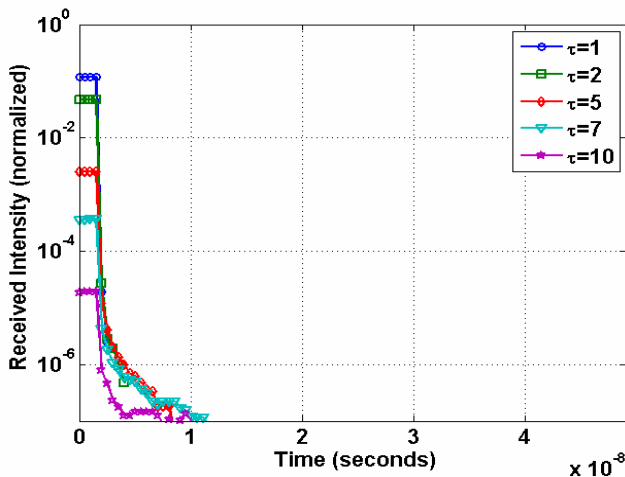


Figure 3. Impulse response of a system with a 20cm diameter receiving aperture for different optical thickness values.

Receiver FOV is determined by the ratio of photo-detector diameter to the lens focal length. Nevertheless photo-detector diameter is proportional to its input capacitance and, hence, inversely proportional to its bandwidth (rate). For a commercial photo-detector, the diameter ranges from 30µm for 10 GB/s to 70µm for 2.5 GB/s [12]. Thus, FOV turns out to be very small for high-speed communications and cloud impulse response reduces to an attenuated impulse. For more details on cloud channel modeling, the reader is referred to [13, 14].

B. Turbulence and Kolmogorov theory

Temperature variations and wind give rise to refractive index fluctuations in different layers of atmosphere. Optical turbulence can be characterized by three parameters: inner scale  $l_0$ , outer scale  $L_0$ , and the structure parameter of the refractive index fluctuations  $C_n^2$  [15]. The well-known Hufnagle-Valley equation models the profile of  $C_n^2$  as:

$$C_n^2(h) = 0.00594(v/27)^2(10^{-5}h)^{10} \exp(-h/1000) + 2.7 \times 10^{-6} \exp(-h/1500) + A \exp(-h/100), \quad (4)$$

where  $h$  is the altitude in meters (m),  $v$  is the rms wind speed in meters per second (m/s), and  $A$  is the nominal value of  $C_n^2(0)$ .  $C_n^2$  is a measure of the strength of turbulence. Variations in the refractive index, give rise to distortion in the wave-front (iso-phase plane), which causes phase perturbations on the receiver plane. Hence, under near field conditions, we only expect to observe phase perturbations. Under far field conditions, bending of the optical rays caused by refraction, along with propagations to the pupil plane make different portions of the wave interfere with one another, causing self-interference. The amplitude variations are caused by these interference elements. In other words, phase perturbations evolve into both amplitude and phase fluctuations as a result of propagation [16]. According to Rytov approximation, amplitude and phase fluctuations resulted from atmospheric turbulence can be modeled as a complex multiplicative factor at each point of the wave-front. For example, the optical field at a distance  $L$  from the transmitter is given by [15]:

$$U(r, L) = U_0(r, L) \exp[\psi(r, L)] = U_0(r, L) \exp[X(r, L) + iS(r, L)] \quad (5)$$

where  $X(r, L)$  represents amplitude fluctuations and  $S(r, L)$  represents phase variations. Also,  $U_0(r, L)$  is the received wave-front under a turbulence-free condition. Using central limit theorem, for long propagation distances through turbulence, it can be shown that  $X$  and  $S$  are homogeneous, isotropic and independent Gaussian random variables [2]. According to equation (5), both amplitude and intensity are log-normally distributed at the pupil plane. However, since we use IM/DD, we need to know variations of the intensity at the focal plane and more specifically, over the small area of a photo-detector.

Depending on the ratio of aperture diameter  $D$  and the atmospheric coherence length (Fried's parameter [15, 16]),  $r_0$ , intensity distribution in the focal plane might be different.

In most previous works, it has been assumed that aperture diameter,  $D$ , is much smaller than the atmospheric coherence length,  $r_0$  [1, 2]. This usually happens when turbulence is relatively weak ( $r_0$  is large) or when there is a practical limitation for increasing the aperture size. In this case, receiver is modeled as a point aperture, collecting an approximately coherent field with a log-normally distributed amplitude fading factor. Due to coherence of the field over this small aperture, Point Spread Function (PSF) of the system remains undistorted.

Under weak turbulence conditions, where Rytov approximation is valid, the *log-irradiance variance*  $\sigma_{\ln I}^2 = 4\sigma_x^2$  ( $\sigma_x^2$  is the *log-amplitude variance*) is approximately equal to the *normalized variance of irradiance* or the *scintillation index*, i.e.,  $\sigma_I^2 \cong \sigma_{\ln I}^2$  [15]. The scintillation indices of plane and spherical waves are given by [1, 2, and 15]:

$$\sigma_I^2 |_{plane} = 2.25k^{7/6} \int_0^L C_n^2(h)(1-h/L)^{5/6} dh, \quad (6)$$

$$\sigma_I^2 |_{spherical} = 2.25k^{7/6} \int_0^L C_n^2(h)h^{5/6}(1-h/L)^{5/6} dh \quad (7)$$

where  $k$  is the wave number. Furthermore, to make sure that the average optical field amplitude is neither attenuated nor amplified, the mean value of log-irradiance is set to  $-\sigma_I^2/2$  [1, 2]. Hence, the PDF of irradiance can be expressed as:

$$f_I(I) = \frac{1}{I\sqrt{2\pi\sigma_I^2}} \exp\left\{-\frac{(\ln(I) + \sigma_I^2/2)^2}{2\sigma_I^2}\right\} \quad (8)$$

The effect of atmospheric turbulence on a system with a point (small) receiving aperture is quite similar to the frequency non-selective flat fading channel in RF communications [17], where multiple paths are not resolved, and hence no pulse broadening is observed. In other words, turbulence manifests itself as a log-normal flat fading coefficient.

We also consider aperture diameters larger than the atmospheric coherence length. This usually happens when turbulence is rather strong (small  $r_0$ ) or the aperture can be made large to combat the amplitude fading. Here, due to aperture averaging effect [1, 2], attributes of intensity fluctuations in the pupil plane are reduced, significantly. However, due to phase aberrations, optical field impinging on the pupil plane breaks up into several spatial modes. Therefore, Point Spread Function (PSF) of the system is distorted. This is very similar to multi-path fading in the RF communications, where the impulse response is broadened and dispersed. Note that, PSF is the spatial system impulse response and dispersion takes place in spatial domain, rather than temporal which is the

case for RF communications. Broadening of the PSF and its random wandering over photo-detector active area give rise to signal attenuation and fading. Therefore, even though we use intensity modulation, we need to take the phase distortions into account. The impact of PSF distortion is more severe on optical imaging systems, where the spatial impulse response determines the image resolution and quality. Here, we assume that receiver is equipped with a perfect tracking system, which can compensate for beam wanders. Nonetheless, phase aberrations can not be removed by simple tracking and hence, should be compensated for by other techniques. Adaptive-Optics is one such technique. However, the focus of this paper is on effectiveness of MIMO configurations in compensating for both amplitude and phase fluctuations.

Phase perturbations are usually approximated by a thin phase screen, the power spectrum of which is given by the Kolmogorov or von Kàrmàn model. According to the Kolmogorov theory, assuming isotropic and homogenous turbulence, the power spectral density of refractive index fluctuations can be expressed as [15, 16]:

$$\Phi_n(\kappa) = 0.033C_n^2\kappa^{-11/3}, 1/L_0 < \kappa < 1/l_0 \quad (9)$$

where  $\kappa$  is the spatial wave number. Hence, the power spectrum of phase fluctuations is represented as:

$$\Phi_p(k) = 0.023r_0^{-5/3} |\kappa|^{-11/3}, 1/L_0 < \kappa < 1/l_0 \quad (10)$$

where  $r_0$  is the atmospheric coherence length (Fried parameter) and is approximated as:

$$r_0 = 0.185 \left[ \frac{4\pi^2}{k^2 \int_0^L C_n^2(h)(1-h/L)^{5/3} dh} \right]^{3/5} \quad (11)$$

This parameter is a measure of coherence radius of the optical field. As turbulence becomes stronger,  $r_0$  decreases. Since coherence length of the field is proportional to  $r_0$ , if two receivers are by  $r_0$  apart, they observe virtually independent versions of the signal. The phase structure function can be defined as [15, 16]:

$$D_p(|r|) = 6.88 \left( \frac{|r|}{r_0} \right)^{5/3} \quad (12)$$

The most popular way of generating a Kolmogorov phase screen is via Fast Fourier Transform (FFT). In this method, a Gaussian white noise process is multiplied by the square root of spectrum in (10) and then Fourier transformed to generate a random phase screen with the desired power spectrum. Ideally, the phase screen must be as large as the outer scale of turbulence  $L_0$ , with sample-spacing as small as  $l_0$ . However,  $L_0$  is several orders of magnitude larger than  $l_0$ , and hence a large number of samples is required for this method to work properly. If the number of samples is not sufficient, due to abrupt change of power spectrum in the vicinity of

origin, low frequencies can not be properly represented in the phase screen. New techniques, such as sub-harmonics method, or random mid-point displacement algorithm have been proposed to overcome these limitations [18-20]. In this paper, we use the random mid-point displacement algorithm to generate the phase screens. This algorithm, exploits the self-similar and fractal nature of phase fluctuations to generate phase screens of desired structure function.

The primary effect of phase perturbations is broadening and distortion of the PSF. In other words, depending on the severity of turbulence, energy collected by lens cannot be concentrated on a small focal spot and the photo-detector may not be able to collect all of it. Fig. 4 shows the PSF in the absence of turbulence. Moreover, Fig. 5 and Fig. 6, demonstrate the PSF for relatively weak and moderate turbulence levels, respectively. From these figures, one can see that as  $D/r_0$  increases, PSF becomes more distorted. Furthermore, we notice that under relatively weak turbulence conditions, the beam is just slightly tilted and the center of the PSF is no longer at the focal point. However, in relatively moderate turbulence beam breaks up and multiple bright spots can be observed. Note that, as long as Rytov variance (or scintillation index) is less than 1, the Rytov approximation is valid and turbulence is generally considered to be weak [15]. Throughout this paper, we assume this approximation is valid and the terms “weak turbulence” and “strong turbulence” are relative.

We conclude this section by the following remarks:

- Clouds and aerosols attenuate and disperse the laser pulse. Since we are using receivers of small FOV, only LOS component can be observed and in the channel impulse response, clouds appear as an attenuation factor, due to scattering.
- Atmospheric turbulence, introduces both amplitude and phase variations into the pupil plane optical field.
- When  $D/r_0$  is small, receiver is modeled as a point aperture and amplitude variations give rise to log-normal intensity fading. However, due to coherence of optical field, PSF is not distorted.
- When  $D/r_0$  is large, aperture averaging is observed. However, several spatial modes impinge upon the collecting lens and PSF is distorted. The random, time variant distortion of PSF changes the amount of light absorbed by photo-detector and hence gives rise to attenuation and fading of the signal.
- If  $D/r_0$  increases due to strength of turbulence (reduction in  $r_0$ ), variance of intensity fluctuations may increase beyond a level that can be compensated completely by aperture averaging. In this case, both amplitude and phase fluctuations contribute to fading.

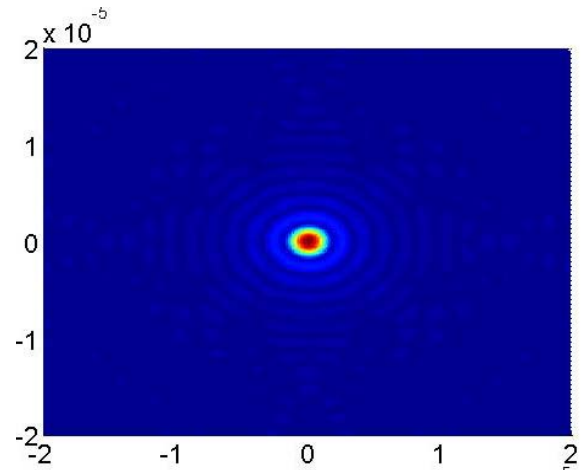


Figure 4. Point spread function in the absence of turbulence.

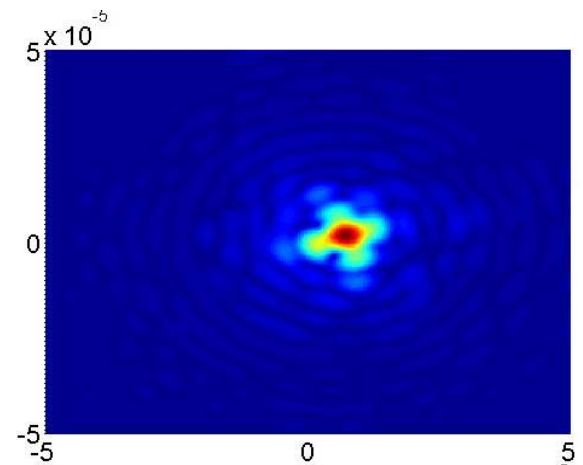


Figure 5. PSF in the presence of weak turbulence  $D/r_0 \approx 5$

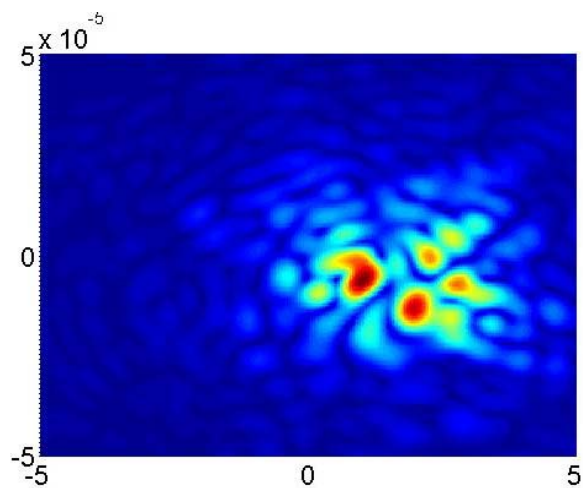


Figure 6. PSF in the presence of moderate turbulence  $D/r_0 \approx 20$ .

### III. SYSTEM DESIGN

The enormous bandwidth promised by FSO communications is available only under clear, turbulence-

free atmospheric conditions, where there is no dispersion to bring about ISI, and power loss is virtually zero. However, this is not a realistic situation and to exploit the great potentials of FSO communications, proper measures should be used in transmitter and receiver designs. MIMO communications systems are proven to be effective in RF or Infrared (IR) fading channels. In this section, we present possible designs for MIMO FSO communications systems. The ability of multiple transmitters and receivers in combating fading is conditioned on reception of uncorrelated copies of the signal. As a result, transmit and receive apertures must be placed at least one correlation distance ( $r_0$ ) apart. For atmospheric channel this requirement can be easily met since correlation distance (atmospheric coherence length) is about 20 cm under good visibility conditions and often drops to 2-4 cm during the day [21].

Depending on the ratio of receiving aperture diameter and atmospheric coherence length,  $D/r_0$ , and strength of turbulence, aperture averaging effect may be observed. In other words, if  $D > r_0$  and  $\sigma_I^2$  is sufficiently small, intensity variations do not contribute much to signal fading. If on the other hand  $\sigma_I^2$  increases due to relative strength of turbulence, intensity fluctuations may be observed despite the aperture averaging. Furthermore, if  $D \gg r_0$ , PSF is no longer a single spot in the focal point and collected energy is distributed all over the focal plane. Since relative strength of turbulence, and hence  $r_0$ , is time variant, one should consider all the above-mentioned possibilities in the receiver design. As a result, we cannot count on aperture averaging effect to totally overcome the amplitude fading.

When  $D/r_0 < 1$ , deleterious effects of turbulence emerge as a log-normal intensity fading. In this case, substituting a single receiver with properly-spaced multiple receivers of smaller sizes provides spatial diversity and hence mitigates the fading. When  $D/r_0 > 1$ , using multiple receivers of smaller sizes has the benefit that each of these receivers collects a smaller number of spatial modes. As a result, their PSFs are less distorted compared to a single large receiver.

The outputs of multiple receivers can be combined using either Equal Gain Combining (EGC) or Maximal Ratio Combining (MRC). Replacing the single high power transmitter with multiple transmitters of the same total power may increase the system diversity order and hence is expected to improve the performance.

Fig. 7a shows a Single-Input Single-Output (SISO) system operating in presence of clouds and turbulence. In Fig. 7b, the SISO system is replaced by a 2x2 MIMO system. Sum of the areas of smaller multiple receiving apertures is equal to the area of single aperture receiver. Moreover, total transmitted power is the same for SISO and MIMO transmitters. A single photo-detector is used in the focal plane of each receiving aperture, to ensure that in background noise-limited reception, the total

collected noise is the same for both systems. As a result, transmitters and receivers should be placed such that, in turbulence-free conditions, a single photo-detector in the focal plane of each receiver can collect the signals from all transmitters. The combiner in MIMO system can be either EGC or MRC. SISO transmitter and receiver can be replaced by an arbitrary number of sub-apertures, and as long as the total transmitted power and area of receivers are kept the same, comparison of two systems is fair. In our simulations, we consider the 2x2, 3x3, 4x4, and 7x7 MIMO configurations. Note that in a 7x7 MIMO design, a single receiving aperture of SISO configuration is replaced with seven smaller apertures, each of which receiving the signal from a slightly different direction (spatial mode) [22]. This is very similar to the fly-eye receiver used in indoor optical communications [23].

In the next section, the BER performance of SISO and MIMO systems are compared for different signal-to-noise ratio (SNR) values, considering amplitude and phase perturbations.

#### IV. RESULTS

In this section, we compare the BER performance of SISO and MIMO optical communications systems in presence of turbulence. Effectiveness of multi aperture receivers in mitigating log-normal amplitude fading has been discussed in some of the earlier works [1-3]. We show how transmit and receive diversity helps to overcome both amplitude and phase fluctuations. To this end, a vertical optical link of 2 km length is considered. Laser beam propagation through turbulent atmosphere is simulated using Fourier Optics and thin phase screens.

To investigate the effectiveness of aperture-averaging phenomenon, BER performance of single-aperture receivers of various diameters is calculated via simulation. More specifically, single-aperture receivers of diameters 5, 10, and 20 cm are considered and for different atmospheric turbulence strength levels, incident wave is perturbed by simulated phase screens. An ensemble average of BER performance is calculated based on PSF patterns and amplitude fading factors. Then, for the same set of phase screens, BER performance of MIMO system with the same total transmit power and receiving area is calculated for both MRC and EGC scenarios. Aperture-averaging is taken into account by reducing the variance of intensity fluctuations according to the ratio of aperture diameter and atmospheric coherence length [15, 24].

Fig. 8 shows BER performance under relatively weak turbulence conditions, where  $A = 1.7 \times 10^{-13}$ ,  $v = 21$  m/s,  $r_0 = 5$  cm, and scintillation index is  $\sigma_I^2 = 0.089$ . SISO receiving aperture diameter is set to 5 cm and a MIMO system of the same total transmitted power and receiving aperture area is considered. Note that in this case,  $D/r_0 = 1$ , and hence, turbulence manifest itself, mostly as log-normal amplitude fading. However, PSF is not distorted as much. Due to superiority of MRC over EGC, and in order to avoid confusion, only BER performance

curves of MRC MIMO systems are plotted in Figs. 8 to 11.

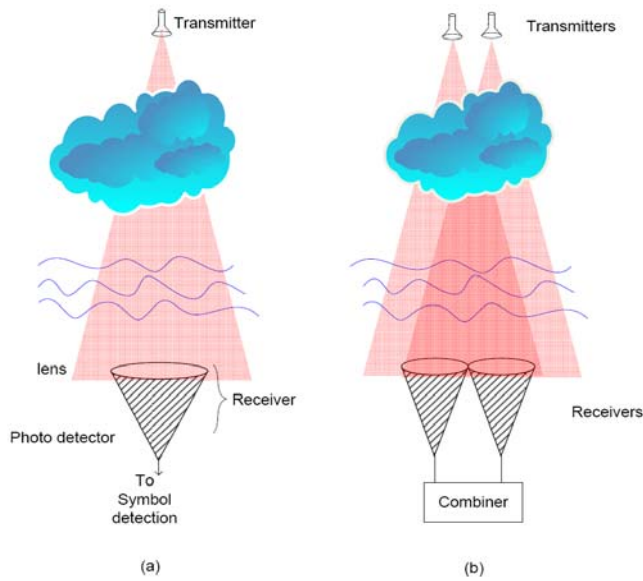


Figure 7. (a) SISO and (b) MIMO communications systems.

One can see that, most performance improvements are due to aperture averaging, which reduces the scintillation variances for both SISO and MIMO receivers. Having multiple transmitters in MIMO system provides more diversity and MIMO system performs slightly better than the SISO counterpart. Furthermore, by increasing the number of apertures, BER performance curves become closer to the AWGN channel performance.

Fig. 9 shows BER performance under relatively stronger turbulence conditions, where  $A = 1.7 \times 10^{-12}$ ,  $v=21$  m/s,  $r_0 = 1.4$  cm, and scintillation index is  $\sigma_I^2 = 0.8$ . Here again, SISO receiving aperture diameter is set to 5 cm and a MIMO system of the same total transmitted power and receiving aperture area is considered. Since aperture diameter is small and scintillation index is relatively large, aperture averaging is not effective and BER performance is still far from that of AWGN. Furthermore, by increasing the number of apertures, MIMO system performance improves compared to the SISO counterpart.

By increasing the aperture diameter to 10 cm (Fig. 10), both SISO and MIMO systems show performance improvements, due to aperture averaging effects. However, this improvement is more significant for the MIMO system, as PSF distortion has started to emerge.

One may expect that if receiver diameter is increased to 20 cm, more improvements may be observed. However, due to deleterious effects of phase distortion, this is not the case. In other words, by increasing the aperture diameter, we are increasing the  $D/r_0$  ratio and hence a larger number of spatial modes impinge on the pupil. As a result, PSF becomes more distorted.

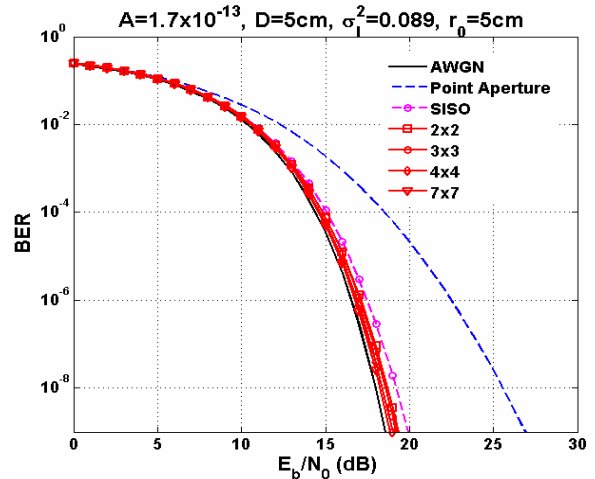


Figure 8. Comparison of SISO and MIMO BER performance in weak turbulence condition,  $A = 1.7 \times 10^{-13}$ ,  $v=21$  m/s and  $\sigma_I^2=0.089$  (single aperture diameter is 5 cm).

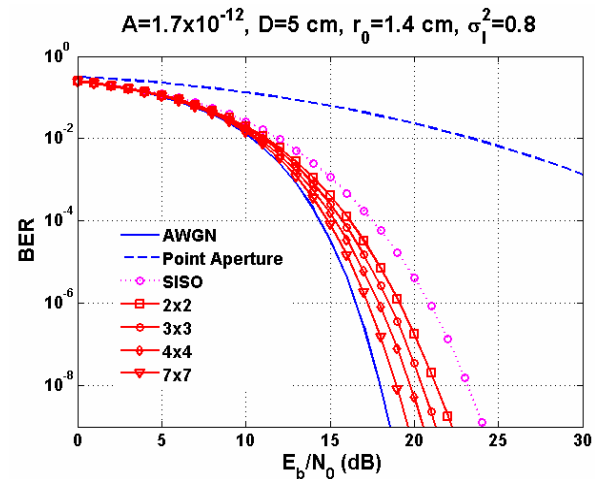


Figure 9. Comparison of SISO and MIMO BER performance in strong turbulence condition,  $A = 1.7 \times 10^{-12}$ ,  $v=21$  m/s and  $\sigma_I^2=0.8$  (single aperture diameter is 5 cm).

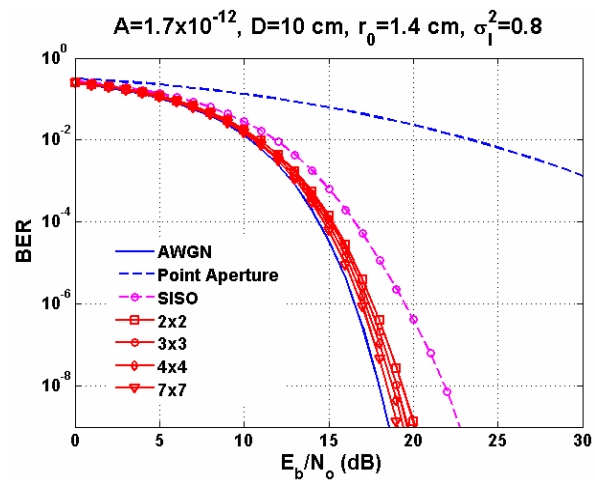


Figure 10. Comparison of SISO and MIMO BER performance in strong turbulence condition,  $A = 1.7 \times 10^{-12}$ ,  $v=21$  m/s and  $\sigma_I^2=0.8$  (single aperture diameter is 10 cm).

Fig. 11 demonstrates the BER curves for this scenario. Due to smaller diameters of receivers, the 7x7 MIMO system is more robust to this kind of fading. However, performance of SISO and MIMO systems with smaller number of apertures are more or less degraded, since PSF distortions reduce the amount of signal collected by photo-detectors. Another observation is that there is an optimum ratio of  $D/r_0$  that enables us to benefit from aperture-averaging, without giving rise to severe PSF distortion. However, atmospheric coherence length,  $r_0$ , is highly variable, and hence a system of fixed receiving aperture area can not guarantee the optimum performance all the time. A MIMO system with a large number of branches, on the other hand, provides diversity to combat log-normal amplitude fading effects. Furthermore, due to its smaller receiving apertures (compared to a SISO system), it experiences less PSF distortions and fading associated with offset of received power from the photo-detector area.

Here, we have assumed that multiple received copies of signal are attenuated independently due to log-normal amplitude fading. If there is some correlation between the paths of diversity branches, MIMO system performance will degrade. In fact [25] reports less MIMO gain using transmit diversity due to correlation between the traveled path through the atmosphere. Hence, there is less motivation for introducing MIMO FSO links in comparison to RF links, as used in a rich scattering transmission environment.

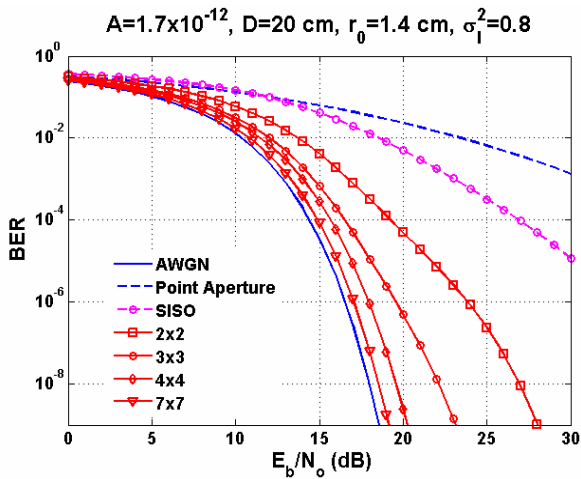


Figure 11. Comparison of SISO and MIMO BER performance in strong turbulence condition,  $A = 1.7 \times 10^{-12}$ ,  $v = 21$  m/s and  $\sigma_l^2 = 0.8$  (single aperture diameter is 20 cm).

### V. CONCLUSIONS

FSO communications, though having great potentials in providing high data rate communications, faces major challenges when operating in a turbulent, cloudy atmosphere. While clouds and aerosols attenuate laser pulses and spread them both temporally and spatially, turbulence perturbs wave-front and introduces amplitude

and phase variations in the wave collected by receiving aperture. In this paper, we assume that only LOS component of the scattered beam can be collected by the lens due to small FOV of receiver. Hence, clouds and aerosols are modeled as a plain attenuation factor. Turbulence-induced amplitude variations are modeled by log-normal fading and we use phase screens to account for phase front perturbations.

We show that aperture averaging can reduce intensity fluctuations, significantly. Furthermore, due to transmit diversity, MIMO systems perform slightly better than an equivalent SISO system in the presence of log-normal amplitude fading. When phase perturbations become significant due to relative strength of turbulence, MIMO system is proven to be more robust to PSF distortions and intensity fading. MIMO design can provide this performance improvement because of diversity and the fact that PSFs of its smaller receivers are less distorted compared to a single large aperture. In other words, the ratio of aperture diameter to the atmospheric coherence length is smaller than that of a single larger aperture. Furthermore, since atmospheric coherence length is usually in the order of a few centimeters, correlation between the signals received by these smaller apertures is negligible. However, if there is correlation between the paths of multiple beams, one might not observe much excess gain by exploiting multiple transmitters [25].

### REFERENCES

- [1] S. M. Navidpour, M. Uysal, M. Kavehrad, "BER Performance of Free-Space Optical Transmission with Spatial Diversity," *IEEE Transactions on Wireless Communications*, Vol. 6, No. 8, pp 2813-2819, Aug. 2007.
- [2] X. Zhu and J. M. Kahn, "Free-Space Optical Communication through Atmospheric Turbulence Channels," *IEEE Trans. on Communications*, Vol. 50, No. 8, pp 1293-1300, Aug. 2002.
- [3] E. J. Lee and V.W.S. Chan, "Part 1: Optical Communication Over the Clear Turbulent Atmospheric Channel Using Diversity," *IEEE Journal on Selected Areas in Communications, Optical Communications and Networking*, Vol. 22, No. 9, pp 1896-1906, Nov 2004.
- [4] A. Belmonte, A. Comerón, J. A. Rubio, J. Bará, and E. Fernández, "Atmospheric- turbulence-induced power-fade statistics for a multiaperture optical receiver," *Applied Optics*, Vol. 36, No. 33, pp 8632-8638, Nov. 1997.
- [5] S. Karp, R. Gagliardi, S. Moran, L. Stotts, *Optical Channels*, Plenum, New York, 1988.
- [6] F. G. Smith, *The Infrared & Electro-optical Systems Handbook: Atmospheric Propagation of Radiation*, Vol. 2, SPIE PRESS, pp 99-100, 1993.
- [7] D. Deirmendjian, "Scattering and Polarization Properties of Water Clouds and Hazes in the Visible and Infrared," *Appl. Opt.*, Vol. 3, No. 2, pp 187-196, Feb. 1964.
- [8] B. Y. Hamzeh, *Multi-rate Wireless Optical Communications in Cloud Obscured Channels*, Ph.D. Thesis, Pennsylvania State University, December 2005.
- [9] R. M. Gagliardi and S. Karp, *Optical Communications*, 2<sup>nd</sup>ed, John Wiley, New York, pp 289-290, 1995.
- [10] E. A. Bucher, "Computer simulation of light pulse propagation for communication through thick clouds," *Applied Optics*, Vol. 12, No. 10, pp 2391-2400, Oct. 1973.

- [11] A. Ishimaru, *Wave Propagation and Scattering in Random Media*, Volume II: Multiple scattering, turbulence, rough surfaces and remote sensing, Academic Press, New York, pp 253-325, 1978.
- [12] D.M. Jeganathan, and D.P. Ionov, "Multi-Gigabits-per-second Optical Wireless Communications," [http://www.freospaceoptic.com/WhitePapers/Jeganathan%20\(Optical%20Crossing\).pdf](http://www.freospaceoptic.com/WhitePapers/Jeganathan%20(Optical%20Crossing).pdf).
- [13] B. Hamzeh and M. Kavehrad, "OCDMA coded Free Space Optical Links for Wireless Optical Mesh Networks," *IEEE Trans. on Communications*, Vol. 52, No. 12, pp 2165-2174, Dec. 2004.
- [14] Z. Hajjarian, J. Fadlullah, M. Kavehrad, "Use of Markov Chain in Atmospheric Channel Modeling of Free Space Laser Communications," *Proceedings of the IEEE MILCOM*, pp 1-7, Nov. 2008.
- [15] L. C. Andrews, R. L. Phillips, and C. Y. Hopen, *Laser Beam Scintillation with Applications*, SPIE Press, pp 1-66, 2001.
- [16] M. C. Roggemann, and B. M. Welsh, *Imaging Through Turbulence*, CRC Press, Boca Raton, FL, pp 57-122, 1996.
- [17] John G. Proakis, *Digital Communications*, 4<sup>th</sup> Ed, McGraw Hill, 2001.
- [18] R. Lane, A. Glindemann, and J. Dainty, "Simulation of a Kolmogorov phase screen," *Waves in Random media*, Vol. 2, pp 209-224, July 1992.
- [19] E. M. Johansson and D. T. Gavel, "Simulation of stellar speckle imaging," in *Amplitude and Intensity Spatial Interferometry II*, J. B. Breckinridge, ed., *Proc. SPIE*, Vol. 2200, pp 372-383, March 1994.
- [20] B. J. Herman and L. A. Strugala, "Method for inclusion of low-frequency contributions in numerical representation of atmospheric turbulence," in *Propagation of High-Energy Laser Beams through the Earth's Atmosphere*, *Proc. SPIE*, Vol. 1221, pp 183-192, Jan. 1990.
- [21] V. Vilnrotter and M. Srinivasan, "Adaptive Detector Arrays for Optical Communications Receivers," *IEEE Transactions on Communications*, Vol. 50, No. 7, pp 1091-1097, July 2002.
- [22] Z. Hajjarian, and M. Kavehrad, "Using MIMO Transmission in Free Space Optical Communications in presence of clouds and turbulence," *Proc. SPIE*, Vol. 7199, pp 71990V 1-11, Feb. 2009.
- [23] G. Yun, M. Kavehrad, "Indoor Infrared Wireless Communications Using Spot Diffusing and Fly-Eye Receivers," *Canadian Jour. on Elect & Comp. Eng.*, Vol. 18, No. 4, pp 90-96, 1993.
- [24] L. C. Andrews, R. L. Phillips, *Laser Beam Propagation Through Random Media*, 2<sup>nd</sup> ed, *SPIE Press*, pp 477-532, 2005.
- [25] I. I. Kim, H. Hakakha, P. Adhikari, E. J. Korevaar, and A. K. Majumdar, "Scintillation reduction using multiple transmitters," *Proc. SPIE.*, Vol. 2990, pp 102-113, Feb. 1997.

**Zeinab Hajjarian** is a Ph.D. student in the Electrical Engineering Department, Center for Information and Communication Technology Research (CICTR), The Pennsylvania State University, University Park, PA.

**J. Fadlullah** is a Ph.D. student in the Electrical Engineering Department, Center for Information and Communication Technology Research (CICTR), The Pennsylvania State University, University Park, PA.

**Mohsen Kavehrad** received his Ph.D. degree from Polytechnic University (Brooklyn Polytechnic), Brooklyn, New

York, November 1977 in Electrical Engineering. Between 1978 and 1989, he worked on telecommunications problems for Fairchild Industries, GTE (Satellite and Labs.) and AT&T Bell Laboratories. In 1989, he joined the University of Ottawa EE Department, as a full professor. Since January 1997, he has been with the Pennsylvania State University EE Department as W.L. Weiss Chair Professor and founding Director of Center for Information and Communications Technology Research. He is a Fellow of the IEEE for his contributions to wireless communications and optical networking. He received 3 Bell Labs awards for his contributions to wireless communications, the 1990 TRIO feedback award for a patent on an optical interconnect, 2001 IEEE VTS Neal Shepherd best paper award, 3 IEEE Lasers and Electro-Optics Society best paper awards between 1991-95 and a Canada NSERC PhD-thesis award in 1995, with his graduate students for contributions to wireless systems and optical networks. He has over 300 published papers, several book chapters, books, and patents in these areas. His current research interests are in wireless communications and optical networks. He is a former Technical Editor for the *IEEE Transactions on Communications*, *IEEE Communications Magazine* and the *IEEE Magazine of Lightwave Telecommunications Systems*. Presently, he is on the Editorial Board of the *International Journal of Wireless Information Networks*. He served as the General Chair of leading IEEE conferences and workshops. He has chaired, organized and been on the advisory committee for several international conferences and workshops.